

# Lithium niobate-tantalate mixed crystals electronic and optical properties calculated from *first principles*

A. Riefer, S. Sanna and W.G. Schmidt  
Lehrstuhl für Theoretische Physik,  
Universität Paderborn  
33098 Paderborn, Germany

**Abstract**—The electronic and optical properties of the mixed-crystal system lithium niobate–tantalate has been calculated from *first principles*. Based on density functional theory we calculate the electronic properties including quasiparticle effects within the GW approach. The optical response including electron-hole attraction effects is obtained from the solution of the Bethe-Salpeter equation. While the band gap increase with increasing tantalum content and shows some bowing, a nearly linear dependence of the optical birefringence on the stoichiometry is calculated.

**Keywords:** LNT, LiNbO<sub>3</sub>, LiTaO<sub>3</sub>, birefringence, BSE, GWA

## I. INTRODUCTION

Lithium niobate (LN) and lithium tantalate (LT) are two isomorphic ferroelectric materials sharing several common properties. While LN is the most important electro-optic material typically used in optical modulators, acousto-optic devices, optical switches for gigahertz frequencies, laser frequency doubling, nonlinear optics, Pockels cells, optical parametric oscillators or Q-switching devices for lasers, LT serves as a LN replacement for shorter wavelength.

Mixed LN-LT crystals (LNT, LiNb<sub>1-x</sub>Ta<sub>x</sub>O<sub>3</sub> crystals) have recently attracted the attention of the scientific community since they offer the possibility to tune the physical properties by varying the composition. Lithium niobate-tantalate is one of the simplest ferroelectric mixed crystals, which shows quite unusual physical properties. In particular, the existence of a composition with zero birefringence at room temperature is unique in ferroelectric nonlinear-optical materials. Indeed within this composition the crystal is optical isotropic and yet electrically polar [1,2].

Despite the huge potential in electro-optic and acousto-optic devices and the extensive use of LN and LT, relatively little is known about the mixed-crystal system lithium niobate–tantalate [3]. This is mainly due to the difficulty to grow compositionally homogeneous crystals with traditional methods such as the Czochralski growth from a lithium rich melt. In fact, despite the isomorphism of the compounds and the similar radii and valence of Ta and Nb, the large separation of the solid-liquid lines in the LN-LT phase diagram makes the crystal growth across the composition range a technically demanding task. However, the growth of homogeneous crystals by several techniques has been demonstrated recently.

Recently we have shown that the optical properties of LN can be accurately calculated starting from density-functional theory by solving the Bethe-Salpeter equation (BSE) using quasi-particle corrections from the GW approach (GWA) [4].

Here we present calculations for the LNT electronic and optical properties including the optical birefringence. The applied methods are briefly explained in the section II. In section III we present the results.

## II. METHODOLOGY

The calculation of the optical and electronic properties proceeds within the following three steps: (i) We use density functional theory in generalized gradient approximation (DFT-GGA) to determine the structural and electronic ground state of the LNT crystals. Therefore, to simulate LNT crystals with the compositions  $x = 0.0, 0.25, 0.5, 0.75,$  and  $1.0$  we apply a  $1 \times 1 \times 2$  rhombohedral super-cell containing 20 atoms. The structural parameters are obtained *ab-initio* by relaxing the ionic coordinates and fitting the Murnaghan equation of state [5] (see Ref. [21]). (ii) The electronic quasiparticle spectrum is obtained within the GWA to model the exchange-correlation self-energy, and finally (iii) the Bethe-Salpeter equation (BSE) is solved for coupled electron-hole excitations [6–8], thereby accounting for the screened electron-hole attraction and the unscreened electron-hole exchange [9–11].

In detail, starting from *first-principles* projector augmented wave (PAW) calculations, we use the VASP implementation of the DFT-GGA [12, 13]. A  $4 \times 4 \times 4$  k-point mesh is applied to sample the Brillouin zone. The electron wave functions are expanded into plane waves up to an energy cutoff of 400 eV. The mean-field effects of exchange and correlation in GGA are modelled using the PW91 functional [14]. In the second step, we include electronic self-energy effects by a perturbative solution of the quasiparticle equation, where the GGA exchange and correlation potential is replaced by the nonlocal and energy-dependent selfenergy operator  $\Sigma$ . Using the implementation described in [15] we calculate  $\Sigma$  in the  $G_0W_0$  approximation [16] from the convolution of the single-particle propagator  $G$  and the dynamically screened Coulomb interaction  $W$ . 704 electronic bands per LN/LT unit-cell are included in the calculation of the self-energy operator.

The electron-hole interaction is taken into account in the third step. The two-particle Hamiltonian

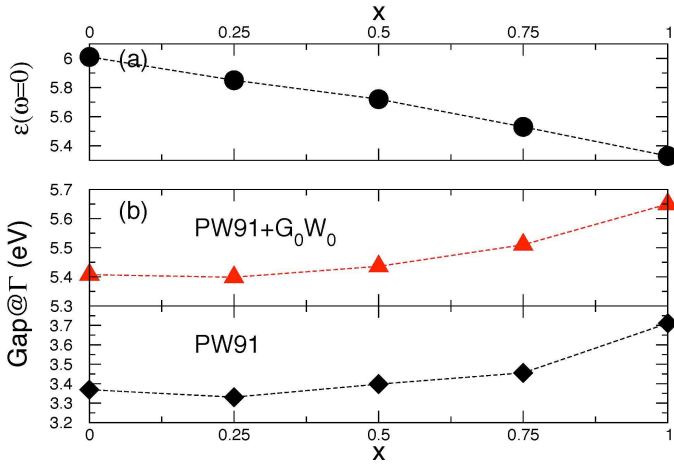


Figure 1. (a) Dielectric constant  $\epsilon_\infty=\epsilon(\omega=0)$  for LNT crystals with  $x=0.0, 0.25, 0.5, 0.75, 1.0$  calculated within IPA. (b) Band gap at the center of the Brillouin zone  $\Gamma$  calculated either within DFT-PW91 (black diamonds) or  $G_0W_0$  approach (red triangles).

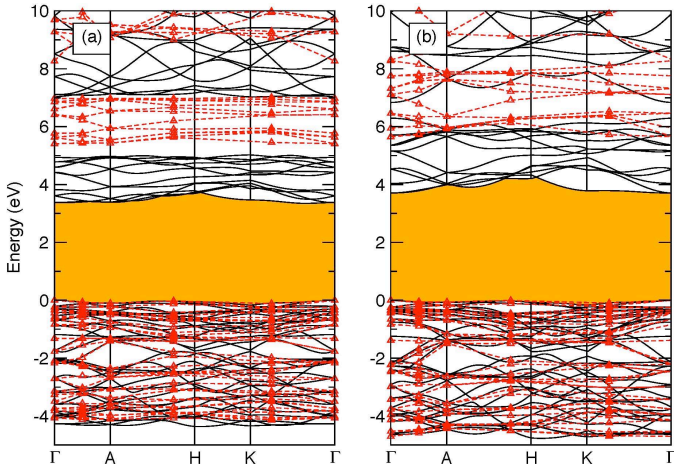


Figure 2. Electronic band structure of (a) LN and (b) LT calculated within DFT-PW91 (solid lines, black) and  $G_0W_0$  approach (red triangles) given with respect to the valence band maximum. The notation of the high symmetry points is explained in Ref. [20]. Dashed lines guide the eye. The fundamental band gap is shown in orange.

$$H_{vck,v'c'k'} = (\epsilon_{ck} - \epsilon_{vk})\delta_{vv'}\delta_{cc'}\delta_{kk'} + 2 \iint d\mathbf{r}d\mathbf{r}' \phi_{ck}^*(\mathbf{r})\phi_{vk}(\mathbf{r})\bar{v}(\mathbf{r}-\mathbf{r}')\phi_{c'k'}(\mathbf{r}')\phi_{v'k'}^*(\mathbf{r}') - \iint d\mathbf{r}d\mathbf{r}' \phi_{ck}^*(\mathbf{r})\phi_{c'k'}(\mathbf{r})W(\mathbf{r},\mathbf{r}')\phi_{vk}(\mathbf{r}')\phi_{v'k'}^*(\mathbf{r}'), \quad (1)$$

describes the interaction of pairs of electrons in conduction states  $|c\mathbf{k}\rangle$  and holes in valence states  $|v\mathbf{k}\rangle$  [6,7,16]. The diagonal first part is given by the quasiparticle energies obtained in GW approximation. The second, the electron-hole exchange term, where the short-range part of the bare Coulomb potential  $\bar{v}$  enters, reflects the influence of local fields. Finally, the third part, which describes the screened electron-hole attraction, is calculated using a model dielectric function as proposed by Bechstedt *et al.* [17]. Thereby we use the values

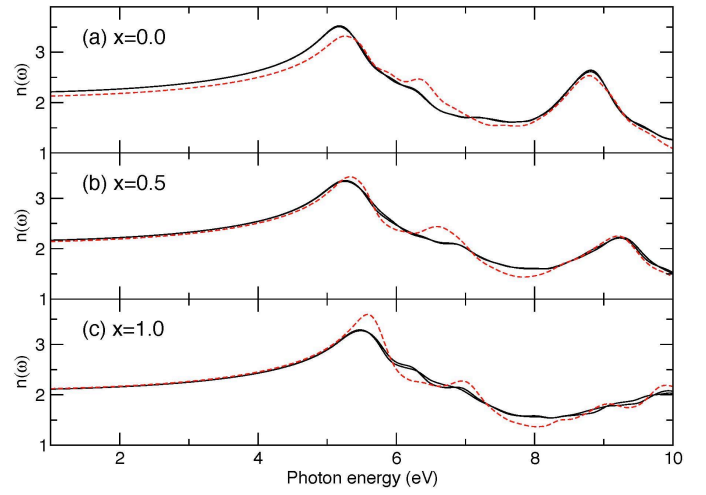


Figure 3. Refractive index obtained from the optical response calculated by solving the BSE (with  $G_0W_0$  corrections) for LNT crystals with  $x=0.0, 0.5, 1.0$  for ordinary (solid, black) and extraordinary (dashed, red) polarization.

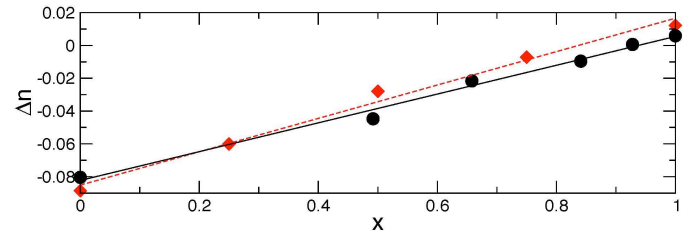


Figure 4. Calculated birefringence  $\Delta n$  (diamonds) for LNT crystals for  $\lambda=632.8$  nm ( $\omega=1.96$  eV). Circles denote experimental values obtained by Wood *et al.* [2].

$\epsilon_\infty$  shown in Fig. 1, obtained from optical independent-particle approximation (IPA) calculations, as input parameter. For the actual calculation of the polarizability, we use the time-evolution implementation described in [18, 19].

### III. RESULTS

Based on the equilibrium structures determined within DFT (see also Ref. [21]) the electronic structure and optical response is calculated. In Fig. 1 the behavior of the averaged dielectric constants  $\epsilon_\infty=\epsilon(\omega=0)$  and the  $G_0W_0$  band gap at the  $\mathbf{k}$ -point  $\Gamma$  are shown. Going from LN to LT the calculations show that the former is reduced moving nearly linear with  $x$  starting at 6.01 and ending at 5.33. The  $G_0W_0$  gap instead, is heightened starting at 5.41 eV for LN and ending at 5.65 eV for LT. For  $x=0.25$  we find a broad a minima for the gap, which is even more visible in the DFT-PW91 calculation. In the main, the inclusion of self-energy effects leads to a rough enhancement of the gap of about 2 eV for LNT crystals.

Fig. 2 compares the electronic band structures for LN and LT. As can be expected from the structural isomorphism, in general, the band structures are similar. However, for LT the dispersion of the electronic bands is larger.

The values for the dielectric constant and the direct gap at  $\Gamma$  for LN are in agreement with our previous study Ref. [4], apart

from a slight deviation due to the increased lattice constants compared to Ref. [4] (see Ref. [21]) and slightly different numerical parameters. An additional discussion about the LN band gap is given in Ref. [4] either. For LT and mixed LNT crystals, however, we are not aware of comparable *ab-initio* calculations or experimental data.

Fig. 3 shows the refractive index  $n(\omega)$  obtained from the optical response calculated within BSE applying  $G_0W_0$  corrections for LNT crystals. Two features at about 5 - 8 eV and 9 - 11 eV can be found in the spectra. For increasing tantalum amount this features are slightly blue-shifted due to the increasing band-gap. The optical birefringence  $\Delta n = (n_e - n_o)$ , where  $n_e/n_o$  denotes the refractive index parallel/perpendicular to  $c$ , appear to be almost constant for photon energies below 5 eV and changes its sign with increasing  $x$  from negative to positive. For  $\lambda = 632.8$  nm ( $\omega = 1.96$  eV) values for  $\Delta n$  are given in Fig. 4. They depend nearly linear on  $x$ . The data show good agreement with measurements obtained by Wood *et al.* [2] for a temperature of 20°C.

#### IV. ACKNOWLEDGMENTS

We gratefully acknowledge financial support from the DFG as well as supercomputer time provided by the HLRS Stuttgart and the Paderborn PC<sup>2</sup>.

#### REFERENCES

- [1] A. Bartasyte, A. M. Glazer, F. Wondre, D. Prabhakaran, P. A. Thomas, S. Huband, D. S. Keebl, and S. Margueron, "Growth of  $\text{LiNb}_{1-x}\text{Ta}_x\text{O}_3$  solid solution crystals", *Mat. Chem. and Phys.*, vol. 134, pp. 728-735, June 2012.
- [2] I. G. Wood, P. Daniels, R. H. Brown, and A. M. Glaze, "Optical birefringence study of the ferroelectric phase transition in lithium niobate tantalate mixed crystals:  $\text{LiNb}_{1-x}\text{Ta}_x\text{O}_3$ ", *J. Phys.: Condens. Matter*, vol. 20, pp. 235237-235242, May 2008.
- [3] D. Xue, K. Betzler, and H. Hesse, "Dielectric properties of lithium niobate-tantalate crystals", *Sol. Stat. Comm.*, vol. 115, pp. 581-585, Aug. 2000.
- [4] A. Riefer, S. Sanna, A. V. Gavrilenko, W. G. Schmidt, "Linear and nonlinear optical response of  $\text{LiNbO}_3$  calculated from first principles", *ISAF/PFM 2011*, doi: 10.1109/ISAF.2011.6014156, to be published.
- [5] F. D. Murnaghan, "The compressibility of media under extreme pressures", *Proc. Nat. Acad. Sci. USA* vol. 30, pp. 244-247, Sept. 1944.
- [6] S. Albrecht, L. Reining, R. DelSole, and G. Onida, "Ab Initio Calculation of Excitonic Effects in the Optical Spectra of Semiconductors", *Phys. Rev. Lett.*, vol. 80, pp. 4510-4513, May 1998.
- [7] L. X. Benedict, E. L. Shirley, and R. B. Bohn, "Optical Absorption of Insulators and the Electron-Hole Interaction: An Ab Initio Calculation", *Phys. Rev. Lett.*, vol. 80, pp. 4514-4517, May 1998.
- [8] M. Rohlfing and S. G. Louie, "Excitons and Optical Spectrum of the  $\text{Si}(111)-(2 \times 1)$  Surface", *Phys. Rev. Lett.*, vol. 83, pp. 856-859, July 1999.
- [9] L. J. Sham and T. M. Rice, "Many-Particle Derivation of the Effective-Mass Equation for the Wannier Exciton", *Phys. Rev.*, vol. 144, pp. 708-714, April 1966.
- [10] W. Hanke and L. J. Sham, "Local-field and excitonic effects in the optical spectrum of a covalent crystal", *Phys. Rev. B*, vol. 12, pp. 4501-4511, Nov. 1975.
- [11] W. Hanke and L. J. Sham, "Many-particle effects in the optical spectrum of a semiconductor", *Phys. Rev. B*, vol. 21, pp. 4656-4673, May 1980.
- [12] P. E. Blöchl, "Projector augmented-wave method", *Phys. Rev. B*, vol. 50, pp. 17953-17979, Dec. 1994.
- [13] G. Kresse and J. Furthmüller, "Efficient iterative schemes for ab initio total-energy calculations using a plane-wave basis set", *Phys. Rev. B*, vol. 54, pp. 11169-11186, Oct. 1996.
- [14] J. P. Perdew and Y. Wang, "Accurate and simple density functional for the electronic exchange energy: Generalized gradient approximation", *Phys. Rev. B*, vol. 33, pp. 8800-8802, June (1986).
- [15] M. Shishkin and G. Kresse, "Implementation and performance of the frequency-dependent GW method within the PAW framework", *Phys. Rev. B*, vol. 74, p. 035101, July 2006.
- [16] M. S. Hybertsen and S. G. Louie, "Electron correlation in semiconductors and insulators: Band gaps and quasiparticle energies", *Phys. Rev. B*, vol. 34, pp. 5390-5413, Oct. 1986.
- [17] F. Bechstedt, in *Festkörperprobleme / Advances in Solid State Physics*, edited by U. Rössler (Vieweg, Braunschweig/Wiesbaden, 1992), Vol. 32, p. 161.
- [18] W. G. Schmidt, S. Glutsch, P. H. Hahn, and F. Bechstedt, "Efficient  $O(N^2)$  method to solve the Bethe-Salpeter equation", *Phys. Rev. B*, vol. 67, p. 085307, Feb. 2003.
- [19] P. H. Hahn, W. G. Schmidt, and F. Bechstedt, "Bulk Excitonic Effects in Surface Optical Spectra", *Phys. Rev. Lett.*, vol. 88, p. 016402, Dec. 2001.
- [20] W.G. Schmidt, M. Albrecht, S. Wippermann, S. Blankenburg, E. Rauls, F. Fuchs, C. Rödl, J. Furthmüller, and A. Hermann, "LiNbO<sub>3</sub> ground- and excited-state properties from first-principles calculations", *Phys. Rev. B*, vol. 77, pp. 035106-035112, Jan. 2008.
- [21] S. Sanna, A. Riefer, S. Neufeld, and W.G. Schmidt, G. Berth, A. Widhalm, and A. Zrenner, "Vibrational fingerprints of  $\text{LiNbO}_3$ - $\text{LiTaO}_3$  mixed crystals", *ISAF ECAPD PFM 2012 contribution BM174*